Journal of Molecular Liquids 371 (2023) 120937

Contents lists available at ScienceDirect

Journal of Molecular Liquids

journal homepage: www.elsevier.com/locate/molliq

Characterization of eutectic mixtures of sugars and sugar-alcohols for cryopreservation

Adam Joules [a,*], Tessa Burrows [a,1], Peter I. Dosa [b,2], Allison Hubel [c,3]

[a] Department of Biomedical Engineering, University of Minnesota, Minneapolis 55455, USA
[b] Department of Medicinal Chemistry, Institute for Therapeutics Discovery and Development, University of Minnesota, Minneapolis 55455, USA
[c] Department of Mechanical Engineering, University of Minnesota, Minneapolis 55455, USA

ARTICLE INFO

Article history:
Received 16 August 2022
Revised 10 November 2022
Accepted 27 November 2022
Available online 29 November 2022

Keywords:
Natural deep eutectic systems
Water activity
Molar excess volume
Thermal analysis
Raman spectroscopy

ABSTRACT

Natural Deep Eutectic Systems (NADES) composed of sugar and sugar alcohols have been studied and applied in a variety of biological applications. Understanding their interaction with water across dilution and temperature is inherently important for maximizing the utility of NADES. Herein a wide range of sugar:sugar-alcohol molar ratios were synthesized and characterized by viscosity, molar excess volume, differential scanning calorimetry, water activity, and confocal Raman cryomicroscopy. NADES were found to have greater viscosity, reduced heat of fusion, greater absolute molar excess volume, lower water activity, and stronger hydrogen bonding of water than non-NADES mixtures. This is hypothesized to be due to cumulatively stronger hydrogen bonding interactions between components in pure and diluted NADES with the strongest interactions in the water-rich region. This work provides useful data and further understanding of hydrogen bonding interaction strength for a wide range of molar ratios in pure to well-diluted forms.

1. Introduction

Deep eutectic systems (DES) are characterized by strong hydrogen bond donor (HBD) and hydrogen bond acceptor (HBA) interactions [1,2]. These mixtures have a lower melting point than any of the their individual components. Common HBAs include choline chloride and sugars, while common HBDs include urea and glycerol. Glyceline, for example, is a 1:2 molar ratio of choline chloride and glycerol that has been well characterized in both pure and diluted with water forms in the literature [3-5]. Interactions between the components of DES have been investigated with nuclear magnetic resonance (NMR), neutron scattering and x-ray diffraction as well as in molecular dynamics studies [6]. Other common characterization includes viscosity, density, and differential scanning calorimetry [7,8]. The definition of a DES is generally taken as a solvent in which (1) the components mix forming a transparent liquid and (2) the liquid has a melting point lower than any involved component.

DES from natural components, or NADES, also meet the definition above but the components are from natural sources such as metabolites, sugars, amino acids, sugar alcohols [9]. Common NADES involve a sugar as the hydrogen bond acceptor and glycerol as the hydrogen bond donor such as a 1:30 molar ratio of trehalose and glycerol [6]. NADES often have high viscosity and density compared to other solvents, which is attributed to strong hydrogen bonding as studied with NMR [10]. Their value over other DES include higher sustainability, easy and inexpensive preparation, and low toxicity [11].

These solvents are often diluted with water to facilitate their application with biomolecular and biological systems. Such dilution can drastically change the physical properties and stability of NADES as the system interactions are altered. Three regimes have been described as water is added to a DES: water in a DES, hydration of the DES network, and DES components in aqueous solution [9]. Water in NADES can qualify as NADES but would be more appropriately defined as a ternary NADES with HBA:HBD:Water. When the interactions are further solvated or hydrated the eutectic point molar ratio may not be maintained as components are not necessarily stoichiometrically distributed to these other structures [12]. This can change the solvent properties in a complex manner as the components bond more favorably to the

* Corresponding author at: University of Minnesota, 312 Church St. SE, 7-105 Nils Hasselmo Hall, Minneapolis, MN 55455, USA.
E-mail addresses: juelf002@umn.edu (A. Joules), burro139@umn.edu (T. Burrows), pidosa@umn.edu (P. I. Dosa).
[1] University of Minnesota, 312 Church St. SE, 7-105 Nils Hasselmo Hall, Minneapolis, MN 55455, USA.
[2] University of Minnesota, 717 Delaware Bldg, Room 457, Minneapolis, MN 55414, USA.
[3] University of Minnesota, 111 Church St. SE, Minneapolis, MN 55455, USA.

https://doi.org/10.1016/j.molliq.2022.120937
0167-7322/

solvent than to each other [13]. Despite this, the components may not be fully hydrated at a ninety percent molar fraction of water [14]. The transition toward a disrupted network for water on NADES is typically from 50 to 90 molar percent water [15-17]. Characterization of relevant properties from pure NADES to diluted mixtures may provide additional insight and evaluation of component interaction strength with dilution.

NADES have been applied in biopreservation to take advantage of the strong interactions and thermal properties [6,18-21]. Unlike DMSO, a commonly used cryopreservative, NADES have desirable attributes including minimal to no toxicity at high concentrations, ability to modify water and ice from a strong hydrogen bonding network, and formation of biomolecular stabilizing glassy matrices [22]. For example, trehalose, among other carbohydrates, can form glassy matrices with diluents such as sugar alcohols to stabilize biomolecules. The diluent and concentration affects the glass transition temperature and the degree of plasticization of the matrix by the diluent [23]. Water activity, an important yet underutilized property, measures the potential for water to contribute in reactions and phase changes between different solvents and may reflect the ability of NADES to modify water [24].

Potential uses of these NADES include preservation of biologics (e.g., vaccines, proteins, cells, tissue), stabilization of proteins, and using the osmolyte system to modify the properties of biological fluids. Similar NADES have already been applied for DMSO-free cell preservation and outperformed DMSO-based preservation in post-thaw viability and function [19-21,25,26]. A 1:30 molar ratio of a trehalose:glycerol NADES has been used to extend the room temperature storage duration of virus-like particles (VLP) displaying influenza glycoprotein on the particle surface [18]. Additional uses of NADES include "green" extraction and sorption solvents and reaction media for catalyzed and non-catalyzed organic and biological reactions [27]. These latter applications are most suited to pure or minimally diluted NADES.

NADES of amino acids, malic acid, lactic acid, and betaine have been studied and characterized.[10,28-30] NADES with high acidity or containing ammonium molecules can be toxic to cells. [6,30] Sugars and sugar alcohols are osmolytes that are also present in freeze-tolerant species and studied for cryopreservation of cells previously.[31] In this work we synthesized and characterized pure sugar (A) with sugar-alcohol (B) solvents (A:B) of a "high" (1:36) molar ratio and low ratio as limited by solubility of A in B. Pure and water diluted solvents were characterized by density, viscosity, DSC, water activity, and Raman spectroscopy.

2. Materials and methods

2.1. Materials

Trehalose dihydrate (Tre, >99%), glucose (Glu, >99.5%), sorbitol (Sorb, 98%), and choline chloride (ChCl, 98%) were obtained from Sigma-Aldrich. Glycerol (Gly, 99.5%) was obtained from HUMCO, propylene glycol (PG, 99.5%) was obtained from NDL, and Normosol-R was obtained from ICU Medical. All reagents were used as received except for choline chloride, which was heated at 110 °C for three hours and stored in a desiccator prior to use.

2.2. Synthesis and dilution

Samples were prepared by mixing components at the target molar ratios in capped glass vials and heated at 60 °C for at least 12 h. Samples were left to cool at room temperature for at least 72 h prior to visual and microscopic check by polarized optical microscopy for particulates. The low ratio of A:B was found by attempting synthesis of increasingly higher solid (A) content until the solubility limit of A in liquid sugar alcohol (B) was exceeded. The ratio was then slightly increased to obtain a liquid sample. A ratio of 1:36 and the low ratio formed the concentration range for characterization. Pure A:B samples were characterized prior to dilution with Normosol-R ("water", W), an isotonic solution of balanced electrolytes, to A:B weights of 90, 70, 40, and 10 % in solution. Water content provided by trehalose dihydrate (Tre·$2H_2O$) in trehalose based samples was accounted for in characterization data plots.

2.3. Polarized optical microscopy (POM)

10 μL of NADES was pipetted on a glass microscope slide and a #1.5 coverslip placed on top. Transmitted and polarized light inspection was performed at room temperature on a Leica microscope with an eyepiece mounted AmScope 18 megapixel CMOS camera. Image analysis was performed in FIJI (1.53c).

2.4. Viscosity and density

Viscosity measurements were performed with a TA Instruments Discover HR-2 equipped with a standard cup and DIN rotor geometry, a Peltier concentric cylinder system, and a liquid temperature control unit. Rotational mapping, inertia, and friction calibration of the rotor was performed prior to every test. Each sample was run with a constant shear rate of 10 s^{-1} at room temperature (20 °C) after temperature equilibration to within 0.02 °C. Data was logged and analyzed with TA Instruments TRIOS software (5.1.1). Density measurements were performed by carefully weighing 10 mL Gay-Lussac glass bottles of calibrated volumes on a Mettler Toledo analytical balance.

2.5. Molar excess volume

Pure sample density data were converted to molar volumes (V_m) with the following equation.

$$V_m = \frac{1}{\rho_{A:B}} * (x_{A:B} \mathscr{M}_{A:B}) = \frac{1}{\rho_{A:B}} * (x_A \mathscr{M}_A + x_B \mathscr{M}_B) \quad (1)$$

where $\rho_{A:B}$ is the density of pure A:B, $x_{A:B}$ is the molar fraction of A:B, and $\mathscr{M}_{A:B}$ is the molecular weight of A:B. Molar volumes of diluted samples were calculated by:

$$V_m = \frac{1}{\rho_{A:B:W}} * (x_{A:B} \mathscr{M}_{A:B} + x_W \mathscr{M}_W) \quad (2)$$

where x_W is the molar fraction of water and $\mathscr{M}_W$ is the molecular weight of water.

Molar excess volume (V_m^E) was calculated from the measured densities of pure and diluted samples and known sample compositions with the following equation:

$$V_m{}^E = \left(\frac{1}{\rho_{A:B:W}} - \frac{1}{\rho_{A:B,pure}}\right) x_{A:B} \mathscr{M}_{A:B} + \left(\frac{1}{\rho_{A:B:W}} - \frac{1}{\rho_W}\right) x_W \mathscr{M}_W \quad (3)$$

The excess volume is zero at the composition limits of pure A:B and pure water.

2.6. Differential scanning calorimetry

Differential scanning calorimetry (DSC) was performed on a TA Instruments Differential Scanning Calorimeter Q1000. Samples were pipetted into Tzero aluminum hermetic pans (DSC Consumables) with a sample mass of 7–10 mg and then hermetically sealed. The temperature profile is as follows: (1) equilibrate at 40 °C, cool at 10 °C/min to −150 °C, heat at 10 °C/min heating to 60 °C. An empty pan is used as a reference.

Data were analyzed using TA Universal Analysis (4.5A). The exothermic peak on rewarming was used to calculate the melting temperature and heat of fusion. These were determined by using the Sigmoidal Tangential peak integration function to account for a change in baseline before or after the peak. Melting temperature was defined as the onset of the endothermic peak and heat of fusion was defined as the area of the endothermic peak. Glass transition and softening temperatures were determined by differentiating heat flow data with respect to temperature.

2.7. Water activity

An AquaLab CX3 chilled mirror dew point based activity meter was used to measure water activity of pure and diluted samples. 7–10 mLs was added to a sample cup and placed into the instrument where one warm-up reading was taken for each sample type followed by recorded readings after stable test cycles. Ideal, non-interacting water activities were calculated from the Ross and Norrish equations. Derived from the Gibbs-Duhem relationship the Ross equation (eq. (4)) for water activity assumes the components are non-interacting with each other (A:B) and mix completely in water. The final water activity is a product each component's effect on water individually with reasonable accuracy despite its simplicity.

$$Ross\ \ model: a_{w,A:B:W} = a_{w,saline} * a_{w,A:W} * a_{w,B:W} \quad (4)$$

where $a_{w,A:B:W}$, $a_{w,saline}$, $a_{w,A:W}$, $a_{w,A:B}$ are the water activities of the final mixture, of the saline solution used for dilution, of A in water, and B in water respectively. Single component water activities are predicted with the Norrish equation (Eq. (5)) containing an empirical constant.

$$Norrish\ \ equation: a_{w,i:W} = x_W * exp\left[K * (x_i)^2\right] \quad (5)$$

where $a_{w,i:W}$ is the water activity of a component i in water, x_w and x_i are the mole fractions of water and component i respectively, and K is the Norrish constant.

2.8. Raman spectroscopy

Confocal Raman spectroscopy was performed on a WITec Confocal Raman Microscope System Alpha 300R with a UHTS300 spectrometer and a DV401 CCD detector with 600/mm grating and a 532 nm wavelength Nd:YAG excitation laser. The WITec spectrometer was calibrated with a Mercury–Argon lamp. A 100x objective (0.90 NA) were used to focus the 532 nm excitation laser. Laser power at the objective was 10 mW as measured by an optical power meter. Lateral (X-Y) resolution was approximately 0.3 μm based on Abbe's diffraction limit. 1 μL of sample were pipetted onto a four-stage Peltier connected to a temperature controller. A piece of mica was placed on top of the sample to minimize evaporation and sublimation during imaging. Frozen samples were imaged at −10 °C after manual nucleation of ice by briefly touching the sample with a liquid nitrogen cooled needle.

Spectra were obtained by rastering the laser over each pixel with an integration time of 5 s. Raman images were generated by integrating Raman spectra over all pixels for a given wavenumber range for the component of interest. Spectra were normalized in the 800–1400 cm^{-1} region and smoothed with LOESS smoothing. At 100x the field of view is 15x15 μm and 37.5x37.5 μm at 40x. Images were deconvolved using the theoretical point spread function through FIJI (1.53c).

2.9. Statistics

The null hypothesis was defined as no statistically significant difference between any pair of samples or concentrations. One-sample hypothesis tests were performed using a T distribution for DSC measurements with a 95% confidence level. Two-sample t-tests were performed for comparisons between samples for other characterization measurements. ANOVA was corrected for multiple sample comparisons using Tukey HSD and performed for comparisons between multiple samples.

3. Results and discussion

3.1. Synthesis, POM inspection

Three different solids (A) and two liquid sugar alcohols (B) were evaluated in this study. Trehalose (Tre), glucose (Glu), and sorbitol (Sorb) were selected to include a disaccharide, monosaccharide, and a solid form of a sugar alcohol respectively. Glucose can exist in ring and straight chain forms in solution whereas sorbitol, a sweetener, does not form a ring structure. Glycerol (Gly) and propylene glycol (PG) were selected as known sugar alcohols that penetrate cells for cryoprotective benefit but are likely to form NADES and non-NADES solvents given their melting temperatures. Glyceline, a well-studied DES formed from a 1:2 molar ratio of choline chloride and glycerol (ChCl:Gly) was chosen as a benchmark DES for this study [3,4].

Two molar ratios for each A:B component combination were synthesized. The first ratio, 1:36, corresponds to a solid (A) content of about 3 molar or 5 wt%, and was chosen for its similarity to a known Tre:Gly NADES of 1:30. The second ratio depended on the solubility limit of the solid (A) in the liquid sugar alcohol (B) [6]. These ratios are not necessarily the eutectic point composition but may qualify as a NADES from melting point data compared to the components. Table 1 lists these ratios for each A:B combination.

The evaluation of these solvents for NADES behavior is outlined in Fig. 1. In short, the molar ratio was lowered from 1:36 until solutions no longer formed a stable, clear liquid. Stable solvents were then checked under polarized optical microscopy for particulates and then differential scanning calorimetry (DSC) for pure and 10 wt% A:B solvents in saline solution. Glucose achieved a much lower molar ratio, or higher solids content, than trehalose likely due the smaller size of a monosaccharide having an easier solvation into the solvent than a disaccharide. Glucose could achieve 1:10 and 1:6 M ratios in Gly and PG respectively than 1:30 and 1:18 for trehalose respectively. Propylene glycol mixtures could obtain higher solid content than glycerol NADES and sorbitol could reach highest solid content than glucose or trehalose. For 1:2 Sorb:PG, sorbitol comprised 54 wt% of the mixture. While this may indicate a greater tunable range of properties for these two components, this does not necessitate NADES behavior. Pure solvents were further characterized by viscosity, DSC, and water activity with properties summarized in Table 2.

3.2. Viscosity

Dynamic viscosity of solvents was obtained by evaluating response to shear rate (0.1 to 100 s^{-1}) then measuring viscosity at a constant shear (10 s^{-1}). For molar ratio combinations in Table 1, glycerol (Gly) based solvents had a viscosity range from 424 to 7324 mPa·s whereas propylene glycol (PG) based solvents had a range of 5.6 to 123 mPa·s at room temperature. Newtonian behavior was observed for all solvents for shear rates of 0.1 to 100 s^{-1} as well as the glyceline benchmark. Similar viscosity

Table 1
Components and binary ratios of solid (A) and liquid sugar alcohol (B).

A:B Mixture components	Molar ratios
Glyceline, Choline Chloride:Glycerol (ChCl:Gly)	1:2
Trehalose:Propylene Glycol, (Tre:PG)	1:18, 1:36
Trehalose:Glycerol, (Tre:Gly)	1:30, 1:36
Glucose:Propylene Glycol, (Glu:PG)	1:6, 1:36
Glucose:Glycerol, (Glu:Gly)	1:10, 1:36
Sorbitol:Propylene Glycol, (Sorb:PG)	1:2, 1:36
Sorbitol:Glycerol, (Sorb:Gly)	1:5, 1:36

ranges and Newtonian behavior were observed for other NADES at the temperature evaluated in this study [3,10,32]. All solvents show increasing viscosity with greater solids (A) content. In a solid:solid solvent of citric acid (HBD) and sucrose (HBA), the viscosity increased with an increase in HBA mass fraction as seen for these systems indicating more intermolecular hydrogen bonding could also attribute to these high viscosities [33,34]. At the 1:36 molar ratio, the viscosity of Gly solvents are similar, likely overshadowed by the high viscosity of glycerol, whereas the viscosity of PG solvents are significantly different with Tre:PG having the largest viscosity possibly due to trehalose's larger molar mass. Pure glycerol has a greater viscosity than propylene glycol and no A:PG combination had as high viscosity as any A:Gly sample. This is due in part to propylene glycol having one less hydroxyl group available for hydrogen bonding than glycerol.

3.2.1. Versus temperature

Cooling from 20 to −5 °C resulted in a viscosity increase by factors of 3.5 to 21.7. All solvents showed Arrhenius-like behavior (Fig. 2a) and Newtonian behavior. The flow activation energy, E_a, was determined from the Arrhenius model and ranged from 52.4 to 80.5 kJ/mol for Gly and 33.1 to 60.2 for PG based solvents. These ranges agree with the benchmark DES glyceline, as well as similar NADES [3,10,28,35]. Activation energy seemed to depend on the choice of components rather than the molar ratio with the exception of Sorb:PG. The activation energy nearly doubles for the Sorb:PG solvents which could be attributed from the weight percent increase of sorbitol from 6% to 54% from the 1:36 to the 1:2 molar ratio solvents.

3.2.2. With dilution

As water is added, viscosity rapidly and continuously decreases even when crossing the A:B interaction network is disrupted by water (Fig. 2b, c). Water at low content may fit between interstitial spaces or even enhance interaction strength for other properties, but at 90 wt% A:B viscosity drops to about a tenth of pure A:B solvents for Gly and drops by a third for PG solvents. Across dilution there is no differing behavior of NADES vs. non-NADES solvents and Newtonian behavior is still observed. At 40 wt% A:B, Glu:PG, Sorb:PG, and Sorb:Gly are significantly different comparing low vs 1:36 M ratios suggesting differences in viscosity are due to composition and not necessarily NADES behavior. An analysis of the excess viscosity was performed (S1) showing negative excess for NADES solvents and little to no excess for non-NADES solvents.

3.3. Density

Densities of pure and diluted solvents were obtained at room temperature through simple weighing experiment with a calibrated Gay-Lusaac bottle. This data is useful for comparing strength of interactions between components and for the calculation of molar excess volumes (3.4). For combinations in Table 1, glycerol based solvents had a density range of 1.192 to 1.319 g·cm^{-3}, whereas propylene glycol solvents had a range of 1.050 to 1.233 g·cm^{-3} at room temperature (Figure SI 1). These ranges fall within the common range for other reported NADES (1.04 to 1.63) [3,6,33]. Only the 1:2 Sorb:PG solvent had a density greater than any Gly based solvent. Greater densities with glycerol are likely due to the extra hydroxyl group for hydrogen bonding as the density of pure glycerol and propylene glycol are different. All solvents had a greater density with greater solid content (lower A:B ratio) suggesting favorable interactions between components. At the 1:36 molar ratios, trehalose had a significantly greater density for both Gly and PG based solvents likely due to the greater molecular weight of trehalose.

As water is added the density decreases approximately linearly for all solvents, which is consistent with a choline-glucose system

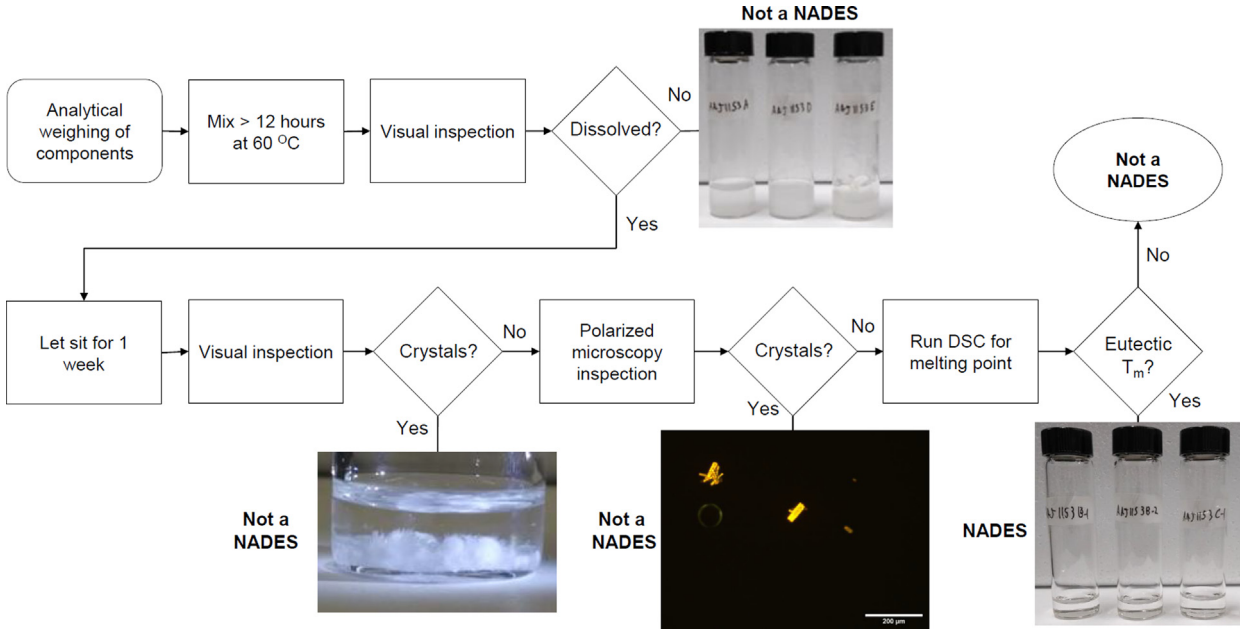

Fig. 1. Flowchart for evaluating NADES or non-NADES combinations of A:B.

Table 2
Summary of properties of pure A:B solvents.

A:B Mixture	Molar ratio	NADES?	[a]Viscosity, μ/ mPa·s	Flow activation, E_a/ kJ·mol^{-1}	[b]Density, ρ/ g·cm^{-3}	Molar volume, V_m/ cm^3·mol^{-1}	[c]Glass transition, T_g/°C	[d]Water activity, a_w/-
ChCl:Gly	1:2	Yes	424	52.4	1.192	90.58	−93.3	0.036
Tre:PG, x_w = 0.061	1:18	No	11.5	37.0	1.109	84.51	−102.2	0.867
Tre:PG, x_w = 0.051	1:36	No	7.5	34.2	1.073	79.29	−105.4	0.894
Tre:Gly, x_w = 0.095	1:30	Yes	2548	70.1	1.287	79.63	−79.5	0.059
Tre:Gly, x_w = 0.051	1:36	Yes	1856	70.5	1.281	78.65	−78.4	0.051
Glu:PG	1:6	No	15.9	40.6	1.141	79.69	−101.1	0.876
Glu:PG	1:36	No	6.0	33.1	1.054	74.88	−105.8	0.898
Glu:Gly	1:10	Yes	4188	75.8	1.305	76.72	−73.8	0.046
Glu:Gly	1:36	Yes	1800	69.8	1.275	74.12	−77.6	0.053
Sorb:PG	1:2	No	123	60.2	1.233	90.38	−82.7	0.855
Sorb:PG	1:36	No	5.6	34.4	1.050	75.17	−105.8	0.928
Sorb:Gly	1:5	Yes	7324	80.5	1.319	81.21	−67.7	0.059
Sorb:Gly	1:36	Yes	1842	68.4	1.271	74.40	−77.9	0.032

*x_w is the mol fraction of water present with trehalose dihydrate.
[a] The standard uncertainty *u* for viscosity is $u(\mu)$ = 0.5 %.
[b] The standard uncertainty *u* for density is $u(\rho)$ = 0.001 g·cm^{-3}.
[c] The standard uncertainty *u* for glass transition temperature is $u(T_g)$ = 0.5 °C.
[d] The standard uncertainty *u* for water activity is $u(a_w)$ = 1 %.

with a greater number of intermediate dilutions (SI 2) [3,16]. Across all dilutions, no differing behavior of NADES and non-NADES solvents was observed. Water is expected to affect the molecular packing of the A:B system and reduce the hydrogen bonding interaction between A:B. Additional water disrupts the A:B solvent until the system is effectively A and B in water. Density decreases with dilution although this disruption does not imply the cumulative strength of interactions of A, B, and W is reduced. Unlike viscosity, the percent change in density was much less with dilution meaning the kinematic viscosity would be driven most by the dynamic viscosity of the pure components. All low vs. 1:36 molar ratios are significantly different across dilution except for Tre:Gly and Glu:Gly (1:30 and 1:10 vs 1:36 respectively) reflecting this method's sensitivity to compare solvents.

3.4. Molar excess volume

Molar excess volume compares the measured or real molar volume of a mixture to the ideal mixture and hence quantifies the non-ideal behavior of mixtures. The molar volume for an ideal mixture is additive and assumes no interaction between the components. At the extremes of composition, the concentrated component mostly interacts with itself and at x = 1.0 the excess volume is zero. In equation (3), the pure density data (Table 1) is used for $\rho_{A:B,pure}$. For trehalose, x_w is plotted as non-zero in Fig. 3 (a-b) from the dihydrate with trehalose.

A negative excess molar volume indicates the solvent is smaller, or denser, than expected for the ideal mixture indicating favorable interactions between components. A positive excess indicates a larger volume than expected indicating repulsive interactions between components. Negative excess volumes were seen for all compositions with more negative excess volume. This suggests the interactions with added water are energetically favorable compared to A:B intermolecular interactions alone. The overall interaction strength continues to increase with added water until a maximum is obtained when the solvent reaches between 90 and 98 molar percent water. Further negative excess volume with added water suggests that the additional interspecies interactions with more water are more favorable than the A:B interactions alone.

None of the solvents reached an absolute excess volume that glyceline has (approx. −0.39 cm^3·mol^{-1}) for any dilution. The Gly solvents did reach the excess volume (approx. −0.34 cm^3·mol^{-1}) of glyceline at high dilution but no PG solvent did. Water is relatively small compared to the A:B components and could occupy interstitial spaces in the A:B network as observed in scattering studies with low dilution [3,36]. This is observed with a slight to moderate negative excess volume at low x_w. Additional water would begin to solvate the A:B network and form hydration structures until the system becomes A and B in an aqueous system. This breakdown point is not clear as the minimum is well within the water-rich region whereas other studies suggest a breakdown between 30 and 50 wt% water (approx. 0.7–0.85 x_w). Additionally, a molecular dynamics study of polar and non-polar DES indicate even at 0.90 x_w not all components are fully hydrated, showing non-ideal mixture properties [14].

Interestingly, while the lower ratio (hollow markers) Gly solvents had reduced excess volume compared to their 1:36 counterparts (solid markers), the opposite was observed for the PG solvents where 1:36 combinations had reduced excess than their lower ratio counterparts. This could point to PG being a non-NADES component in these mixtures where the solid component (A) would be favored over more PG, as in a lower A:B ratio, when diluted. The relatively flat region for Fig. 3B was unexpected given the smooth density data curve obtained across dilution (figure S2) and the closely matching data obtained here compared to previously published molar excess volume for glyceline (ChCl:Gly 1:2) [37]. The variance in the molar excess volume for propylene glycol samples is higher than glycol and the excess volume relies on differences in density rather than the absolute densities. Overall, the PG samples had reduced excess volume than Gly samples and additional concentration datapoints would smooth the dataset for a Redlich-Kister fit.

3.5. Differential scanning calorimetry

Glass transition of pure solvents (Table 2) were obtained with a programmed temperature profile ranging from 60 °C to −150 °C. Enthalpy of fusion, melting and glass transition temperatures were obtained for 10 wt% A:B solvents (Table 3). For pure samples, the only thermal event in the temperature range was a glass transition

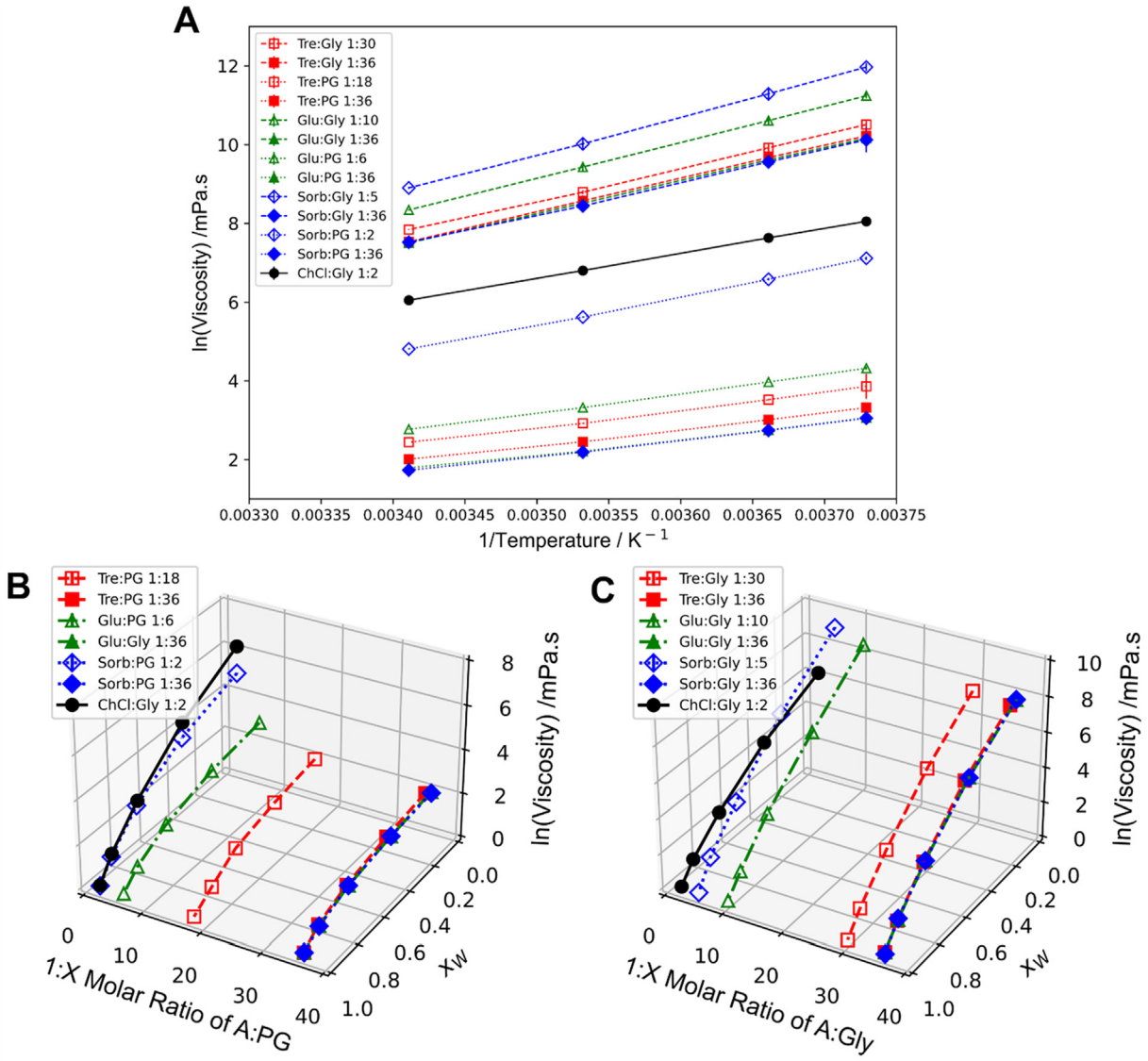

Fig. 2. a) Viscosity vs temperature (20 to −5 °C right to left); b) Viscosity vs dilution of Gly based samples; c) Viscosity vs dilution of PG based samples.

indicating solvent stability and homogeneity (Fig. 4a). Pure glycerol based solvents had a T_g range of −68 to −78 °C and propylene glycol solvents ranged from −83 to −106 °C. It is known that NADES are glass formers but glass formers are not necessarily NADES [13,38]. The addition of solid (A) raised glass transition compared to pure glycerol (−82 °C) or pure propylene glycol (−106 °C), with the lowest glass transition possible driven by the choice of sugar-alcohol. Given the similar structures of components for these samples, the differences in glass transition suggest Gly has greater intermolecular interaction strength with itself than PG. This is likely from the additional hydroxyl group which could also be available for additional A:B interactions.

Differences between 1:36 ratios for the same sugar alcohol (B) were within 1° indicating the solid content controls the glass transition temperature. Without a melting event and no melting point, these solvents could be called low transition temperature liquids (LTTMs). However, for other choline based DES including glyceline, neither ice formation or a melting point is observed but for consistency the solvents are referred to as NADES and non-NADES. Diluted solvents had a freezing and melting event and were used to evaluate the NADES definition.

3.5.1. With dilution

One phase transition (freezing/melting) event and one glass transition event were observed (Fig. 4b). The melting peak was used to determine latent heat of fusion and melting temperature (Table 3). Heat of fusion for glycerol based solvents were lower than propylene glycol based solvents by at least 20 $J \cdot g^{-1}$ meaning the amount of water available for reaction, such as ice formation, is reduced with Gly solvents from greater binding of water. Solvents with trehalose, a known NADES component, had among the lowest latent heat with Gly but the highest latent heat with PG. While reduced heat of fusion and melting point may be beneficial in theory for reducing ice content, a composition with the lowest enthalpy does not imply the optimal composition for cell or biomolecular preservation [20]. Critically, all the Gly solvents and glyceline (1:2 ChCl:Gly) had a melting point lower than water, the lowest melting point component, qualifying them as (NA)DES whereas none of the PG solvents had a melting point lower than PG, the lowest melting point component, disqualifying them as NADES. Even across a 1:2 to 1:36 molar ratio range, none of the PG solvents approached meeting this definition. The Gly solvents here, with a 1:5 to 1:36 eutectic range, may have contain an intermediate eutectic point.

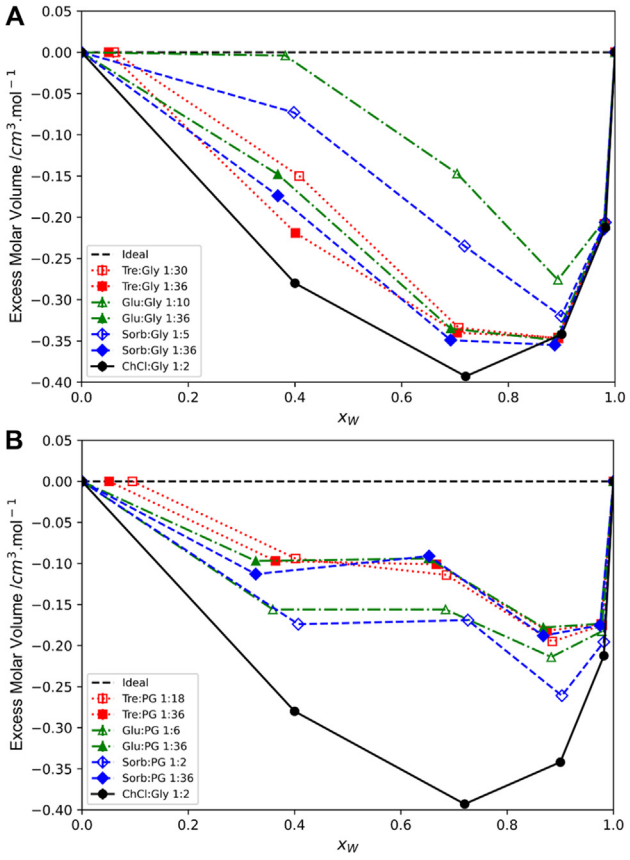

Fig. 3. a) Molar excess volume of Gly based samples; b) Molar excess volume of PG based samples.

Glass transition temperatures increased with greater solid content (lower A:B ratio). PG solvents had the highest T_g overall reaching −74 °C with 1:2 Sorb:PG whereas Gly could only reach −88 °C. Interestingly, the glass transition of PG solvents was raised with the addition of water whereas Gly solvents had lower T_g compared to pure PG and Gly. The glass transition of water, estimated around −137 °C, is much lower than pure Gly and PG but the addition of water had differing effects on them.[39] Water can plasticize the glassy matrix lowering the glass transition temperature and has been noted to decrease for trehalose-water and food materials in general [23,40]. Glycerol has shown antiplasticization behavior in a limited regime whereas propylene glycol shows plasticization to a large degree in other regimes [41].

3.6. Water activity

Activity reflects how tightly bound water is to the system or substrate and can be traced back to the chemical potential (μ) of the mixture. It depends on the interaction strength of solute(s) with water and A:B interactions with water but does not specify molecular structures such as hydration, solvation structure, or equatorial OH groups. However, comparisons can be made with this thermodynamic property and the colligative nature with dilution and different molar ratios. Pure A:B activity is listed in Table 1, though, trace amounts of water are present in these solvents and the low activity approaches the lower limit of detection in the instrument. Therefore, comparisons are made on the 90 wt% A:B solvents (approx. 0.33–0.41 x_w) through dilution to 10 wt% A:B (approx. 0.98 x_w) shown in Fig. 5 (vs. weight percent in S3). Glycerol based solvents ranges from 0.24 to 0.33 a_w whereas propylene glycol solvents ranged from 0.85 to 0.94 a_w at 90 percent A:B and all solvents approached, within 0.02, the activity of the saline solution (0.987). Lower activity was expected for glycerol with a hydroxyl group suggesting water is highly mobile in and out of PG and can more freely contribute to vapor pressure compared to Gly. All low ratio combinations had a higher water activity across dilution until no significant difference in activity was observed with the exception of 1:2 Sorb:PG. This suggests liquid sugar alcohols can bind water better than the solid components as seen with their effect on latent heat, with the exception a solvents with very high sorbitol content (49 wt%), a sugar alcohol itself.

3.6.1. With dilution

Water activity approach that of the saline solution (a_w = 0.987) when diluted to 90 wt% water (about 0.98 x_w). There was no clear breakdown of the A:B network to water as with viscosity, density, and molar excess. Though the change from a curved to approximately linear response for Gly solvents is observed, there is no discontinuity or sudden change that could be explicitly due to this network change. PG solvents had an approximately linear response as the was little water binding ability in the pure solvents. As water is added, activity rises as there is proportionally less A and B to bind water from hydrogen bonding to water. NADES had a non-linear response starting from a lower water activity, a trend seen for other DES and NADES. Non-NADES solvents had an approximately linear change with dilution. At 40 wt% A:B only the low vs. 1:36 ratios of Glu:Gly and Sorb:Gly are significantly different but at 10 wt%, no difference between ratios are observed.

Table 3
Thermal properties of 10 wt% A:B samples in saline solution including melting point, enthalpy of fusion, and glass transition.

A:B Mixture	A:B Molar Ratio	[a]Melting point, T_m/°C	[b]Enthalpy of Fusion, ΔH_{fus}/J·g^{-1}	[c]Glass transition, T_g/°C
ChCl:Gly	1:2	−8.8	207	−106
Tre:PG	1:18	−5.0	254	−89.6
Tre:PG	1:36	−6.0	264	−92.1
Tre:Gly	1:30	−7.8	209	−91.7
Tre:Gly	1:36	−7.9	206	−92.7
Glu:PG	1:6	−5.7	245	−85.8
Glu:PG	1:36	−5.2	240	−95.6
Glu:Gly	1:10	−7.8	204	−91.3
Glu:Gly	1:36	−8.1	207	−94.4
Sorb:PG	1:2	−5.6	241	−74.0
Sorb:PG	1:36	−5.0	253	−95.4
Sorb:Gly	1:5	−6.7	213	−87.9
Sorb:Gly	1:36	−9.1	218	−95.9

[a] The standard uncertainty *u* for melting point is $u(T_m)$ = 0.5 °C.
[b] The standard uncertainty *u* for enthalpy is $u(\Delta H_{fus})$ = 1 %.
[c] The standard uncertainty *u* for glass transition is $u(T_g)$ = 0.5 °C.

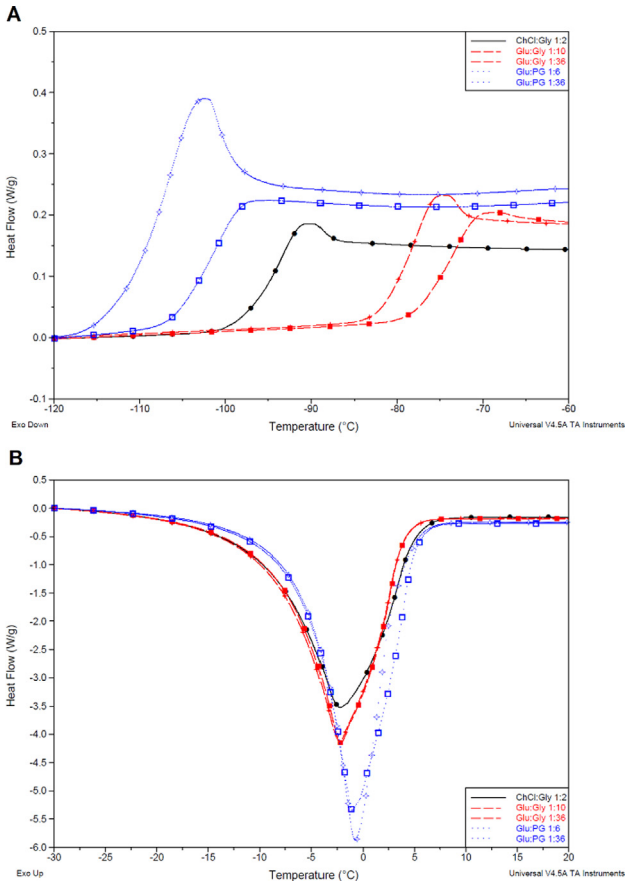

Fig. 4. a) Glass transition events of low and high ratio pure samples and the glyceline benchmark. b) Melting event of 10 wt% A:B samples and the glyceline benchmark.

The Ross and Norrish models were used for predicting the water activity of mixtures and though relatively simple, are a good balance of accuracy and simplicity [42]. Differences in the model and data would reflect additional or reduced chemical potential of water from the interaction between components. The data correlated well with the model at high dilution while NADES showed reduced activity whereas the non-NADES solvents had higher activity. This non-ideal activity was also observed for DES with an added sugar and isopiestic methodology used to determine DES and non-DES behavior [43,44]. There is value in this data for a variety of systems compared to select combinations and limited concentration ranges in the DES and NADES literature [16,43,45,46]. Of the common characterization techniques used for DES, water activity is the most limited dataset as found in a meta-analysis for the modeling and prediction of properties [47,48].

3.7. Low temperature Raman spectroscopy

Further studies were conducted to evaluate these solvents at a reduced temperatures to compare relative hydrogen bonding strengths and response to temperature. Select brightfield and Raman images are shown in Fig. 6 a-c. Only 20 wt% solvents were evaluated at 20 and −10 °C with spectra taken in the non-frozen region of the cooled samples. Raman provides molecular level information of these components during the freezing process enabling comparison of interactions and hydrogen bonding at different temperatures and compositions. Discussion is limited to shifts of components and intramolecular O–H (3200–3800 cm^{-1}) peaks for 20 °C (Fig. 6d) and −10 °C (Fig. 6e) as different instrumentation configurations and environmental factors can affect spectra obtained between studies [49]. The intramolecular O–H band red-shifted for all solvents when cooled suggesting weaker or elongated hydroxyl bonds. Red-shifting is expected, and this band drives the ice formation process during cooling though the non-NADES samples had a slightly greater redshift than NADES. This may be due the water being more mobile in a weaker hydrogen bonding system to form ice compared to water in a stronger NADES bonding system. Additionally, NADES solvents showed consistent blue-shifting behavior as with glyceline by 1 to 3 wavenumbers while non-NADES (propylene glycol) solvents showed slight red-shifting behavior up to 1 wavenumber. This is in agreement with the redshift of NADES intramolecular O–H peaks and may be due to a recombination process where the hydrogen bonding structure moves from strong NADES component-water interactions to favor water-water interactions and form ice [49]. Usual red-shifting from decreasing temperatures can blue-shift in this transition whereas little to no recombination may be required for weaker component-water interactions to form ice in non-NADES solvents. During freezing, solutes are effectively excluded from the ice phase (Fig. 6 a-c) and the concentration of A and B increase and further bind the remaining water. As solvents are further cooled, the increasing solute concentration will eventually bind the remaining water achieving a maximally freeze concentrated system. This composition depends on the components used and their molar ratio implying the advantage of NADES in reaching this state sooner.

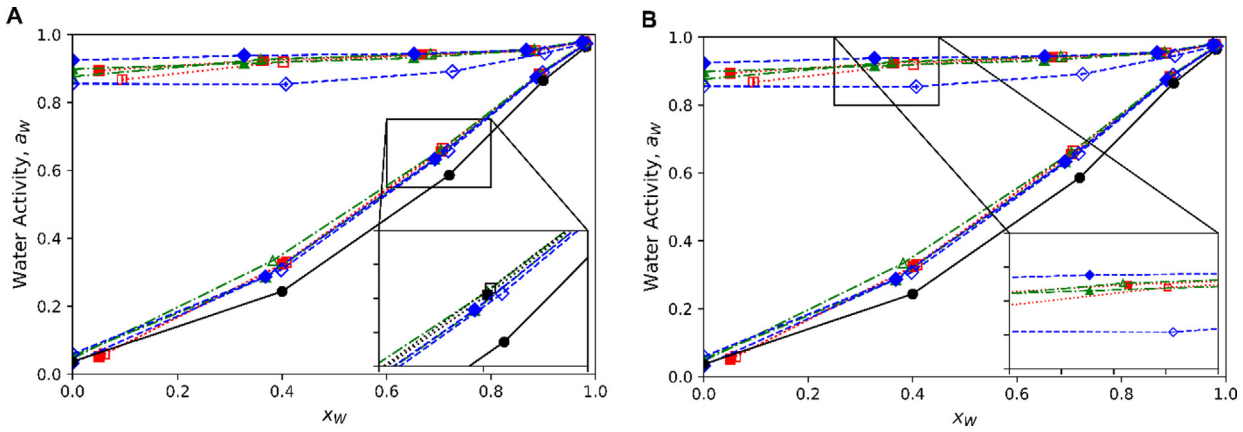

Fig. 5. a) Water activity vs dilution of Gly based samples; b) water activity vs dilution of PG based samples.

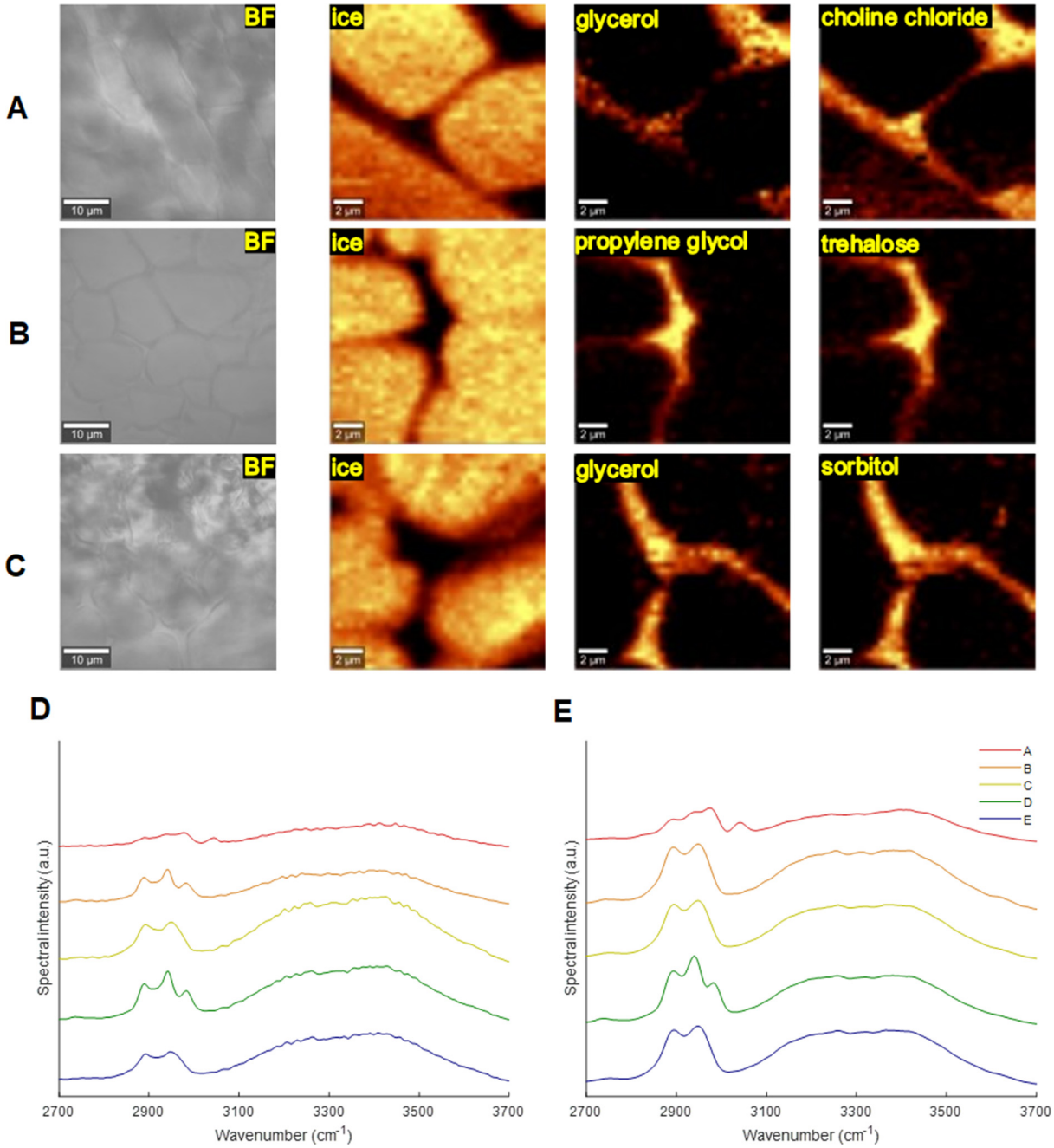

Fig. 6. (a-c) Brightfield images of select frozen NADES samples (scale bar 10 µm) and Raman spectral heat maps (scale bar 2 µm) of ice, sugar alcohol, and component A at −43 °C. a) [Glyceline], b) [1:18 Tre:PG], c) [1:5 Sorb:Gly]. (d-e) OH band spectra at 20 °C and −10 °C for select samples.

4. Conclusions

We explored a wide range of pure A:B compositions with NADES and non-NADES components and characterized their properties across dilution with water. NADES, characterized by strong hydrogen bonding, have greater viscosity and density due to the stronger interactions but both have Newtonian behavior and have an Arrhenius relationship with temperature. The molar excess volume is negative for both, though NADES have much greater non-ideality than non-NADES reaching that of glyceline, a well-studied DES of choline chloride and glycerol (1:2). The breakdown of the greater NADES structure begins at moderate dilution though strong non-ideality is still present at ninety weight percent water. Both NADES and non-NADES have favorable interactions with increased interaction strength with added water, both are glass formers, and show general Raman peak red-shifting behavior when cooled. Water activity is significantly different as non-NADES have higher activity than an ideal model though the relative activities depend on the components chosen.

The additional hydroxyl group contributed to pure glycerol's higher viscosity and melting point than pure propylene glycol. The higher melting point directly contributes to a system qualifying as a NADES and the additional hydroxyl group likely increased the molar excess viscosity for glycerol NADES. The ring (glucose, trehalose) or chain (sorbitol) shape of component A did not impact if an A:B combination was a NADES as the lowest melting point component was the sugar alcohol (B) for all combinations evaluated here. The structure however did affect the obtainable molar

ratio range for each combination. Trehalose, a disaccharide, had a limited solubility of A in B compared to glucose, a monosaccharide. Sorbitol, a chain molecule, could achieve the highest solid content of A in B.

Regarding low temperature and cryopreservation, NADES are hypothetical better solvents for slow freezing with higher glass transition and lower water activity than non-NADES. Cumulative interactions were strongest in the water rich region, approximately ninety mole fraction, suggesting a NADES components in water system and becomes a maximally freeze concentrated solvents during cryopreservation. Greater solid content was beneficial to tune glass transition. Raman spectroscopy showed NADES had stronger component effects on the intramolecular water (O–H) band and components blue-shifted, indicating a hydrogen bonding system recombination, unlike non-NADES. NADES had lower enthalpy of fusion reducing overall ice content though this is not reflective of an optimal formulation for cell preservation.

The solid components studied within form NADES with glycerol. These solvents may however, may be more appropriately called ternary NADES of A:Glycerol:Water within the eutectic range studied given their low water activity and/or strongly negative excess volume with dilution. There is a wide range of possible properties based on the A:Glycerol:Water ratio with the greatest interaction strength in the water rich region and at the eutectic point. There is, however, no clear property indicator explored here for determining strict NADES or non-NADES behavior without comparison to an appropriate ideal model than in the current definition. Further studies with Raman, x-ray diffraction, or neutron scattering could be utilized to explore specific intermolecular interactions of NADES and non-NADES with dilution.

CRediT authorship contribution statement

Adam Joules: Conceptualization, Methodology, Investigation, Formal analysis, Writing – original draft, Visualization. **Tessa Burrows:** Methodology, Investigation, Formal analysis, Writing – original draft, Visualization. **Peter I. Dosa:** Conceptualization, Supervision, Writing – review & editing. **Allison Hubel:** Conceptualization, Supervision, Writing – review & editing.

Data availability

Data will be made available on request.

Declaration of Competing Interest

The authors declare that they have no known competing financial interests or personal relationships that could have appeared to influence the work reported in this paper.

Acknowledgments

This study was funded by the US National Institutes of Health [grant number R01HL154734] and the US National Science Foundation [grant number EEC1941543]. Parts of this work were carried out in the Characterization Facility, University of Minnesota, which receives partial support from the US NSF through the MRSEC [Award Number DMR-2011401] and the NNCI [Award Number ECCS-2025124] programs. We thank Dr. Job Ubbink and Dr. Belal Hasan for thoughtful discussions and expertise on water activity and access to their instrumentation.

Author Statement

The authors of this work, Adam Joules, Tessa Burrows, Peter Dosa, and Allison Hubel, entitles "Characterization of eutectic mixtures of sugars and sugar-alcohols for cryopreservation", here state that all the data present is original, and has never been published or submitted to consideration in any other publication.

Appendix A. Supplementary data

Supplementary data to this article can be found online at https://doi.org/10.1016/j.molliq.2022.120937.

References

[1] A.P. Abbott, G. Capper, D.L. Davies, R.K. Rasheed, V. Tambyrajah, Novel solvent properties of choline chloride/urea mixtures, Chem. Commun. 70–71 (2003), https://doi.org/10.1039/B210714G.
[2] Q. Zhang, K. De Oliveira Vigier, S. Royer, F. Jérôme, Deep eutectic solvents: syntheses, properties and applications, Chem. Soc. Rev. 41 (2012) 7108–7146.
[3] A. Yadav, S. Pandey, Densities and viscosities of (choline chloride + urea) deep eutectic solvent and its aqueous mixtures in the temperature range 293.15 K to 363.15 K, J. Chem. Eng. Data 59 (7) (2014) 2221–2229.
[4] F.S. Mjalli, O.U. Ahmed, Characteristics and intermolecular interaction of eutectic binary mixtures: Reline and Glyceline, Korean J. Chem. Eng. 331 (33) (2016, 2015,) 337–343.
[5] O.S. Hammond, D.T. Bowron, K.J. Edler, Liquid structure of the choline chloride-urea deep eutectic solvent (reline) from neutron diffraction and atomistic modelling, Green Chem. 18 (2016) 2736–2744.
[6] V.I.B. Castro et al., Natural deep eutectic systems as alternative nontoxic cryoprotective agents, Cryobiology 83 (2018) 15–26.
[7] A. Paiva, R. Craveiro, I. Aroso, M. Martins, R.L. Reis, A.R.C. Duarte, Natural deep eutectic solvents - Solvents for the 21st century, ACS Sustain. Chem. Eng. 2 (5) (2014) 1063–1071.
[8] E.L. Smith, A.P. Abbott, K.S. Ryder, Deep Eutectic Solvents (DESs) and Their Applications, Chem. Rev. 114 (2014) 11060–11082.
[9] A.S.D. Ferreira et al., Effect of water on the structure and dynamics of choline chloride/glycerol eutectic systems, J. Mol. Liq. 342 (2021).
[10] V.I.B. Castro, F. Mano, R.L. Reis, A. Paiva, A.R.C. Duarte, Synthesis and Physical and Thermodynamic Properties of Lactic Acid and Malic Acid-Based Natural Deep Eutectic Solvents, J. Chem. Eng. Data 63 (7) (2018) 2548–2556.
[11] Y. Dai, J. van Spronsen, G.J. Witkamp, R. Verpoorte, Y.H. Choi, Natural deep eutectic solvents as new potential media for green technology, Anal. Chim. Acta 766 (2013) 61–68.
[12] H. Passos, D.J.P. Tavares, A.M. Ferreira, M.G. Freire, J.A.P. Coutinho, Are Aqueous Biphasic Systems Composed of Deep Eutectic Solvents Ternary or Quaternary Systems?, ACS Sustain Chem. Eng. 4 (2016) 2881–2886.
[13] R. Craveiro et al., Properties and thermal behavior of natural deep eutectic solvents, J. Mol. Liq. 215 (2016) 534–540.
[14] Q. Gao et al., Effect of water concentration on the microstructures of choline chloride/urea (1:2) /water mixture, Fluid Phase Equilib. 470 (2018) 134–139.
[15] M.C. Gutiérrez, M.L. Ferrer, C.R. Mateo, F. del Monte, Freeze-drying of aqueous solutions of deep eutectic solvents: A suitable approach to deep eutectic suspensions of self-assembled structures, Langmuir 25 (10) (2009) 5509–5515.
[16] Y. Dai, G.J. Witkamp, R. Verpoorte, Y.H. Choi, Tailoring properties of natural deep eutectic solvents with water to facilitate their applications, Food Chem. 187 (2015) 14–19.
[17] O.S. Hammond et al., The Effect of Water upon Deep Eutectic Solvent Nanostructure: An Unusual Transition from Ionic Mixture to Aqueous Solution, Angew. Chemie Int. Ed. 56 (2017) 9782–9785.
[18] R. Correia, L. Meneses, C. Richheimer, P.M. Alves, M.J.T. Carrondo, A.R.C. Duarte, A. Paiva, A. Roldão, Improved storage of influenza HA-VLPs using a trehalose-glycerol natural deep eutectic solvent system, Vaccine 39 (24) (2021) 3279–3286.
[19] R. Craveiro et al., Influence of natural deep eutectic systems in water thermal behavior and their applications in cryopreservation, J. Mol. Liq. 329 (2021).
[20] K. Hornberger, R. Li, A.R.C. Duarte, A. Hubel, Natural deep eutectic systems for nature-inspired cryopreservation of cells, AIChE J. 67 (2021) e17085.
[21] R. Li, K. Hornberger, J.R. Dutton, A. Hubel, Cryopreservation of Human iPS Cell Aggregates in a DMSO-Free Solution—An Optimization and Comparative Study, Front. Bioeng. Biotechnol. 8 (2020) 1.
[22] O.S. Hammond et al., Resilience of Malic Acid Natural Deep Eutectic Solvent Nanostructure to Solidification and Hydration, J. Phys. Chem. B 121 (2017) 7473–7483.
[23] J. Ubbink, Structural and thermodynamic aspects of plasticization and antiplasticization in glassy encapsulation and biostabilization matrices, Adv. Drug Deliv. Rev. 100 (2016) 10–26.
[24] M.J. Blandamer, J.B.F.N. Engberts, P.T. Gleeson, J.C.R. Reis, Activity of water in aqueous systems; A frequently neglected property, Chem. Soc. Rev. 34 (2005) 440–458.

[25] K. Pollock et al., Improved Post-Thaw Function and Epigenetic Changes in Mesenchymal Stromal Cells Cryopreserved Using Multicomponent Osmolyte Solutions, Stem Cells Dev. 26 (2017) 828–842.
[26] A. Gertrudes, R. Craveiro, Z. Eltayari, R.L. Reis, A. Paiva, A.R.C. Duarte, How Do Animals Survive Extreme Temperature Amplitudes? the Role of Natural Deep Eutectic Solvents, ACS Sustainable Chem. Eng. 5 (11) (2017) 9542–9553.
[27] Marcus, Y. Deep Eutectic Solvents. Deep Eutectic Solvents (2019) doi:10.1007/978-3-030-00608-2.
[28] I.M. Aroso, A. Paiva, R.L. Reis, A.R.C. Duarte, Natural deep eutectic solvents from choline chloride and betaine – Physicochemical properties, J. Mol. Liq. 241 (2017) 654–661.
[29] L.A. Rodrigues et al., Deep eutectic systems from betaine and polyols – Physicochemical and toxicological properties, J. Mol. Liq. 335 (2021).
[30] M. Hayyan, Y.P. Mbous, C.Y. Looi, W.F. Wong, A. Hayyan, Z. Salleh, O. Mohd-Ali, Natural deep eutectic solvents: cytotoxic profile, Springerplus 5 (1) (2016).
[31] K.B. Storey, J.M. Storey, Molecular physiology of freeze tolerance in vertebrates, Physiol. Rev. 97 (2017) 623–665.
[32] G. García, S. Aparicio, R. Ullah, M. Atilhan, Deep eutectic solvents: Physicochemical properties and gas separation applications, Energy and Fuels 29 (4) (2015) 2616–2644.
[33] L.K. Savi et al., Natural deep eutectic solvents (NADES) based on citric acid and sucrose as a potential green technology: a comprehensive study of water inclusion and its effect on thermal, physical and rheological properties, Int. J. Food Sci. Technol. 54 (2019) 898–907.
[34] A. Mitar et al., Physicochemical Properties, Cytotoxicity, and Antioxidative Activity of Natural Deep Eutectic Solvents Containing Organic Acid, Chem. Biochem. Eng. Q 33 (2019) 1–18.
[35] A. Messaâdi, N. Dhouibi, H. Hamda, F.B.M. Belgacem, Y.H. Adbelkader, N. Ouerfelli, A.H. Hamzaoui, A New Equation Relating the Viscosity Arrhenius Temperature and the Activation Energy for Some Newtonian Classical Solvents, J. Chem. 2015 (2015) 1–12.
[36] F.S. Mjalli, O. Ahmad, Density of aqueous choline chloride-based ionic liquids analogues, Thermochim. Acta 647 (2017) 8–14.
[37] A. Yadav, S. Trivedi, R. Rai, S. Pandey, Densities and dynamic viscosities of (choline chloride + glycerol) deep eutectic solvent and its aqueous mixtures in the temperature range (283.15–363.15) K, Fluid Phase Equilib. 367 (2014) 135–142.
[38] A. Toxqui-Terán, C. Leyva-Porras, Ruíz-Cabrera, M. ángel, P. Cruz-Alcantar, M. Z. Saavedra-Leos, Thermal Study of Polyols for the Technological Application as Plasticizers in Food Industry, Polym. 10 (2018) 467.
[39] S. Capaccioli, K.L. Ngai, Resolving the controversy on the glass transition temperature of water?, J Chem. Phys. 135 (2011).
[40] K. Kouassi, Y.H. Roos, Glass Transition, Water, and Glycerol Effects on Sucrose Inversion in Pullulan-Sucrose Systems, J. Food Sci. 67 (2002) 3402–3407.
[41] R.J. Fong, A. Robertson, P.E. Mallon, R.L. Thompson, The Impact of Plasticizer and Degree of Hydrolysis on Free Volume of Poly(vinyl alcohol) Films, Polym. 10 (2018) 1036.
[42] A. Zuorro, Water Activity Prediction in Sugar and Polyol Systems Using Theoretical Molecular Descriptors, Int. J. Mol. Sci. 22 (2021) 11044.
[43] E. Behboudi, H. Shekaari, M.T. Zafarani-Moattar, Water Activity in Aqueous Solution of Sucrose in the Presence of Some Deep Eutectic Solvents, J. Chem. Eng. Data 66 (2) (2021) 1043–1054.
[44] K.A. Omar, R. Sadeghi, Can isopiestic method predict the formation of deep eutectic solvents?, J Mol. Liq. 333 (2021).
[45] P.J. Smith, C.B. Arroyo, F. Lopez Hernandez, J.C. Goeltz, Ternary Deep Eutectic Solvent Behavior of Water and Urea Choline Chloride Mixtures, J. Phys. Chem. B 123 (2019) 5302–5306.
[46] X. He, A. Fowler, M. Toner, Water activity and mobility in solutions of glycerol and small molecular weight sugars: Implication for cryo- and lyopreservation, J. Appl. Phys. 100 (2006).
[47] G. Gygli, X. Xu, J. Pleiss, Meta-analysis of viscosity of aqueous deep eutectic solvents and their components, Sci. Reports 101 (10) (2020, 2020,) 1–11.
[48] X. Xu, J. Range, G. Gygli, J. Pleiss, Analysis of Thermophysical Properties of Deep Eutectic Solvents by Data Integration, J. Chem. Eng. Data 65 (3) (2020) 1172–1179.
[49] T. Zhan et al., Interaction of solute and water molecules in cryoprotectant mixture during vitrification and crystallization, J. Mol. Liq. 325 (2021).